

Structural Design and Performance Optimization of Perovskite/Organic Tandem Solar Cells

Chenxi Wu

*College of Materials Science and Engineering, Beijing University of Technology, Beijing, China
cwu237@ukey.edu*

Abstract. Single-junction perovskite solar cells have a relatively low upper limit of efficiency, making it difficult to develop them into industrialized photovoltaic cells. To improve efficiency, perovskite tandem solar cells have become a research focus. Among them, perovskite tandem solar cells can meet different performance requirements by adjusting organic materials. In this paper, by comparing key performance and other factors between perovskite-organic tandem solar cells and those of other types of tandem solar cells, the advantages, areas for improvement, and development prospects of perovskite-organic solar cells are summarized. Meanwhile, the organic layer materials in perovskite-organic solar cells, especially Indacenodithieno [3,2-b] thiophene-imidazolecore (ITIC), are summarized, aiming to sort out the development status of perovskite-organic solar cells in recent years and provide some basic information and innovative ideas for future research in this field.

Keywords: Tandem Solar Cells, Perovskite Photovoltaics, Organic Semiconductors, Interconnecting Layer

1. Introduction

The theoretical efficiency of perovskite solar cells (PSCs) in a single-junction configuration is limited to approximately 30%, constrained by the Shockley-Queisser (S-Q) limit [1]. Furthermore, due to the bandgap of perovskite materials (typically 1.5-1.6 eV), they primarily absorb visible light, resulting in the wastage of near-infrared (NIR) photons. This phenomenon significantly impedes the industrialization and large-scale photovoltaic application of PSCs. To overcome this bottleneck, the development of novel solar cell architectures is imperative. Perovskite-based tandem solar cells, which utilize stacked multiple light-absorbing layers to achieve full-spectrum solar energy harvesting, have emerged as a strategic solution. By exploiting the characteristic of different sub-cells absorbing distinct spectral bands, the tandem configuration can reduce thermalization losses and substantially enhance solar energy utilization and the overall power conversion efficiency (PCE) of the cell.

Based on electrical interconnection schemes, tandem solar cells are primarily categorized into two-terminal (2-T) and four-terminal (4-T) configurations. The key distinction lies in that 2-T sub-cells are monolithically series-connected via an interconnecting layer (ICL), whereas 4-T sub-cells are mechanically stacked and possess independent electrical circuits. Owing to its simpler structure

and lower fabrication cost, the 2-T tandem architecture has witnessed significant development in recent years. Current research achievements report a PCE of 34.6% for dual-junction tandem cells [2].

The fundamental structure of a dual-junction tandem solar cell comprises a wide-bandgap top cell, a narrow-bandgap bottom cell, and an interconnecting layer that couples the subcells. Given that the bandgap of perovskite materials can be widely tuned through compositional engineering, perovskite serves as an excellent top-cell material compatible with various narrow-bandgap bottom cells. Current major categories of perovskite-based tandem solar cells include perovskite/silicon (Si) tandems, all-perovskite tandems, perovskite/copper indium gallium selenide (CIGS) tandems, and perovskite/organic tandems. Perovskite/organic tandem solar cells exhibit unique advantages. Firstly, organic semiconductor materials, such as ITIC, offer high tunability, enabling precise bandgap design for efficient NIR light harvesting. Secondly, the intrinsic flexibility of organic materials supports applications in wearable electronics. However, their certified efficiency (23.6%) remains significantly lower than that of perovskite/Si (31.3%) and all-perovskite (24.8%) tandems, primarily attributed to the low charge carrier mobility within the organic layers and interfacial voltage losses [3,4].

This paper summarizes the current development status of organic layer materials—particularly A-D-A type non-fullerene acceptors (NFAs) like ITIC, which have revolutionized charge separation processes through intramolecular charge transfer (ICT) mechanisms. It systematically compares the performance of perovskite/organic tandem solar cells with other tandem configurations and analyzes the advantages as well as the key factors and bottlenecks limiting their efficiency, such as fill factor (FF), stability, and proposes possible future development directions. This study aims to provide a theoretical foundation for optimizing perovskite-organic tandem solar cells and facilitating their industrialization.

2. Structure, materials and performance of perovskite/organic tandem solar cells

2.1. Fundamental structure of perovskite/organic tandem solar cells

A perovskite/organic tandem solar cell comprises three essential components: a wide-bandgap top cell is designed to absorb high-energy photons, whereas a narrow-bandgap bottom cell is intended to capture the low-energy photons transmitted through the top cell. Additionally, an interconnecting layer (ICL) is incorporated to facilitate efficient carrier recombination, while simultaneously permitting the transmission of long-wavelength photons.

A schematic diagram illustrating the composition and operational principle of these components is presented in Figure. 1 [5]. Specifically, the top cell is used to absorb ultraviolet-visible light. Taking advantage of the perovskite materials' characteristics of high light absorption coefficient and excellent carrier transport properties, it efficiently converts high-energy solar energy. As shown in Figure 1 [5], in most perovskite absorption layers, the absorption of light gives rise to the generation of free charge carriers. The interconnecting layer, as a critical functional layer connecting the top and bottom cells, mainly functions to series-connect the sub-cells, suppress electron-hole recombination, and transmit low-energy photons unabsorbed, transferring from the top cell over to the bottom cell. The core function of the organic bottom cell is to absorb near-infrared light unutilized by the top cell in the solar spectrum, forming spectral complementarity with the top cell to achieve efficient utilization of the full solar spectrum.

As observed in Figure 1 [5], in the top cell, free charge carriers in most perovskite absorption layers are generated upon light absorption. In the bottom cell, the primary excited states in organic

semiconductors are strongly bound Frenkel excitons. Unlike the carriers in materials such as perovskites, which can freely separate and migrate, it is exclusively at the donor-acceptor interface that Frenkel excitons can realize charge separation, like a heterojunction composed of the PM6 donor and the ITIC acceptor.

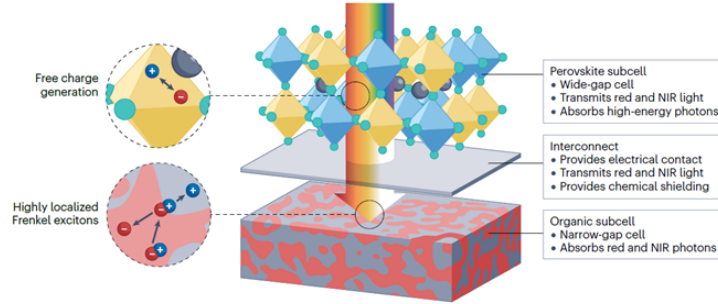


Figure 1. Schematic representation of the fundamental structure of a perovskite/organic tandem solar cell [5]

2.2. Key performance parameters

Perovskite employed as the top-cell material is engineered to harvest high-energy photons within the ultraviolet and visible spectral range (300-700 nm), while simultaneously transmitting lower-energy infrared photons (700-1200 nm) to the underlying organic subcell. This spectral allocation aligns with the approximate absorption bands of both top and bottom subcells, as illustrated in Figure 2 [6]. Such deliberate photon distribution minimizes thermalization losses, constituting a fundamental efficiency advantage for tandem solar cell architectures.

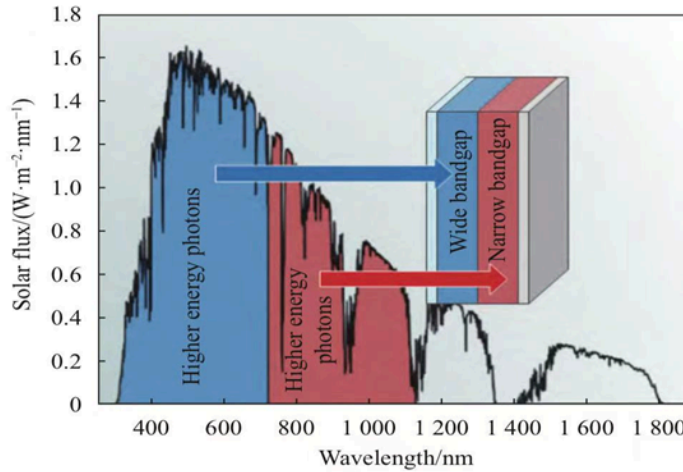


Figure 2. Absorption spectra of wide-bandgap and narrow-bandgap material [6]

To achieve high-efficiency energy conversion, the bandgap energies (E_g) and current outputs of the top and bottom sub-cells must be judiciously matched according to fundamental principles. The target bandgap of the top cell material must satisfy the current matching condition. The core formula can be expressed as [3]:

$$J_{sc}^{top}(E_g^{top}) = J_{sc}^{bottom}(E_g^{bottom}) \quad (1)$$

$$J_{sc} = \frac{q}{hc} \int_0^{\lambda_g} EQE(\lambda) \cdot \lambda \cdot I_{AM1.5G}(\lambda) \cdot d\lambda \quad (2)$$

Where J_{sc} , the short-circuit current density (mA/cm^2). $\lambda_g = \frac{1240}{E_g}$ (nm, eV), J_{sc}^{top} , the short-circuit current density of the top cell (mA/cm^2). J_{sc}^{bottom} , the short-circuit current density of the bottom cell (mA/cm^2) [1,3]. E_g^{bottom} , the known bandgap of the bottom cell. Given that the bandgap of the bottom organic cell in perovskite/organic tandems is typically ~ 1.25 eV, the calculated target bandgap for the top cell material is approximately 1.85 eV. Bandgap engineering of the top perovskite material is commonly achieved through precise control of halide composition. For instance, $CsPb(I_{0.5}Br_{0.5})_3$ incorporates 50% bromide content. Optimization of the top cell bandgap enables complementary absorption with the narrow-bandgap organic bottom cell, maximizing photon utilization across the solar spectrum and enhancing overall device efficiency.

2.3. Classification of organic bottom cell materials

The narrow-bandgap subcell within perovskite-organic tandem solar cells, specifically the organic bottom cell, is designed to harvest infrared photons efficiently. Owing to the vast chemical diversity of organic semiconductors, the selection pool for organic bottom cell materials is extensive. Currently prevalent organic active layer materials encompass the following categories:

Non-Fullerene Acceptors (NFAs) can be structurally categorized into IT-family and Y-family derivatives. IT-family NFAs exhibit less demanding synthetic routes but possess a relatively narrow absorption edge, which inherently limits photocurrent generation. In contrast, Y-family counterparts demonstrate broader spectral coverage while requiring more complex synthesis and exhibiting inferior photostability. Besides, donor Polymers, such as PM6, form bulk heterojunction photovoltaic layers when blended with non-fullerene acceptors.

This section will focus specifically on ITIC, 3,9-bis(2-methylene-(3-(1,1-dicyanomethylene)-indanone))-5,5,11,11-tetrakis(4-hexylphenyl)-dithieno[2,3-d:2',3'-d']-s-indaceno[1,2-b:5,6-b']dithiophene, a representative molecule from the IT-family of non-fullerene acceptors (NFAs) [7]. Prior to the advent of ITIC, fullerene derivatives dominated as electron acceptors. However, the efficiency of the technology plateaued at slightly above 10%, primarily due to the weak absorption of fullerenes across the visible-to-near-infrared spectrum and the inherent difficulty in tuning their frontier orbital energy levels. Distinct from the spherical structure of fullerenes, ITIC features a planar fused-ring donor core as depicted in Figure 3, flanked by electron-accepting end groups. ITIC adopts an acceptor-donor-acceptor (A-D-A) molecular architecture, comprising an electron-donor (D) benzodithiophene (BDT) core and strongly electron-acceptor (A) end groups, typically indenedione (IC) [8].

The A-D-A structure confers significant advantages. The spherical nature of fullerenes promotes tightly bound electron-hole pairs (excitons) susceptible to recombination. Conversely, ITIC's molecular configuration spatially separates electrons and holes, localizing them predominantly on the acceptor (A) termini and the donor (D) core, respectively. This spatial separation facilitates exciton dissociation into free charge carriers under mild conditions. Consequently, ITIC exhibits a pronounced intramolecular charge transfer (ICT) effect upon photoexcitation. Crucially, the ICT state can dissociate directly into free carriers, effectively circumventing recombination losses. The characteristic also lowers the LUMO energy level by approximately 0.3 eV, resulting in a reduced optical bandgap and a concomitant red shift in the absorption spectrum [7,9]. Employing ITIC as an electron acceptor overcame the efficiency limitations inherent to fullerene-based acceptors.

To enhance PCE in organic-containing tandem architectures, two strategic approaches may be implemented: introducing inorganic perovskite materials into organic layers through doping to create hybrid structures, or adding perovskite sub-cells to conventional configurations to form triple-junction devices. These modifications preserve the infrared absorption capabilities inherent to organic components while partially compensating for carrier transport limitations. Significant open-circuit voltage losses have been observed in this system due to energy level misalignment between wide-bandgap perovskites and electron transport layers, despite a successful proof-of-concept demonstration [3]. Nevertheless, this work validates the fundamental viability of triple-junction architectures combining perovskite and organic materials, indicating substantial potential for further development in this domain.

Additionally, the typically poor thermal stability of organic layers presents another efficiency constraint, as molecular chain aggregation or thermal decomposition reduces shunt resistance and consequently diminishes current output and FF [7].

3.2. FF comparison

FF is a dimensionless parameter ranging from 0 to 1, where values closer to 1 indicate that a solar cell operates nearer to its ideal performance with minimal energy losses. This metric is calculated through the equation [12]:

$$FF = \frac{I_{\max} \times V_{\max}}{I_{sc} \times V_{oc}} \quad (3)$$

in which I_{sc} denotes the short-circuit current, V_{oc} represents the open-circuit voltage, and I_{\max} and V_{\max} correspond to the current and voltage values at the maximum power point on the current-voltage curve (I-V). The fill factor exhibits a direct relationship with power conversion efficiency, as expressed by [13]:

$$\eta = \frac{FF \cdot I_{sc} V_{oc}}{p_{in}} \quad (4)$$

where p_{in} stands for incident light power. Consequently, the fill factor serves as a critical performance indicator for evaluating the output power of solar cell.

Perovskite-organic tandem solar cells demonstrate FF between 74.81% and 78.5% [3,11,14]. By comparison, perovskite-silicon tandem devices achieve FF values spanning 69.1% to 79.8% [4,15], all-perovskite tandems attain 78.1% to 81.6% [16,17], and perovskite/CIGS tandems yield 56.6% to 75% [3,18]. These comparative analyses reveal that perovskite-organic tandems display narrower FF fluctuations than CIGS-based devices. The significant variation in CIGS tandems primarily results from inconsistent interfacial contact caused by surface roughness disparities, whereas the constrained FF range in perovskite-organic systems reflects superior process consistency and experimental reproducibility [3,18].

To address FF reduction stemming from the inherently low carrier mobility of organic materials, developing high-mobility acceptors presents a viable solution. For instance, researchers at South China University of Technology employed PM6:Y6 organic layers to elevate charge mobility to 1.5 cm²/(V·s), thereby achieving a 78.5% fill factor [11]. This approach demonstrates that enhancing molecular rigidity through fused-ring structures can effectively improve thermal resilience.

3.3. Stability comparison

Standard stability testing under 1-sun illumination reveals distinct degradation patterns: perovskite-organic tandem cells retain 90% of initial efficiency after 500 hours; perovskite-silicon tandems maintain >96% efficiency following 1,000 hours; all-perovskite devices preserve 94% efficiency over 1,000 hours; and perovskite/CIGS systems sustain over 90% initial performance after 320 hours of continuous operation [3,19-21]. These results confirm the superior thermal stability of perovskite-dominated architectures. As previously noted, the comparatively lower stability of organic-containing tandems originates from the tendency of organic molecular chains to undergo deformation or scission under thermal stress.

Enhancing morphological stability in organic layers could involve incorporating crosslinkers to immobilize molecular chains through covalent bonding. This strategy may draw inspiration from successful grain-boundary engineering in all-perovskite devices, such as the GuaSCN-mediated suppression of crystalline disorder, which is adapted specifically for perovskite-organic systems [22].

3.4. Flexibility potential assessment

The growing demand for wearable electronics and flexible displays necessitates batteries with mechanical flexibility. Flexibility potential – defined as compatibility with flexible electronics manufacturing – depends primarily on two criteria: material compatibility with pliable substrates and adaptability to solution-coating processes. These requirements mandate inherent material flexibility and conformal interfacial contact between functional layers and substrates.

Detailed evaluations indicate fundamental differences: perovskite-silicon tandems lack flexibility due to rigid silicon wafers; all-perovskite devices exhibit excellent flexibility potential since both subcells consist of solution-processable perovskite films under 1 μm thick; perovskite/CIGS configurations show limited flexibility owing to rough CIGS surfaces that require additional interfacial engineering like chemical-mechanical polishing [7]. Perovskite-organic tandems demonstrate exceptional flexibility through organic materials' intrinsic pliability and compatibility with orthogonal solution processing on bendable substrates without rigid supports. Furthermore, their manufacturing compatibility with roll-to-roll techniques enables cost-effective large-area production [9]. Considering these material properties, process adaptability, and scalability factors, perovskite-organic tandems possess the highest flexibility potential among tandem technologies, making them ideal for wearable devices and lightweight power systems.

4. Conclusion

The article introduces the fundamental architecture of perovskite-organic tandem solar cells. Comparative analysis against mainstream technologies—namely, perovskite/silicon, all-perovskite, and perovskite/CIGS tandems—reveals both competitive advantages and persistent challenges for perovskite-organic configurations. Regarding power conversion efficiency, perovskite-organic tandem cells have achieved a certified maximum of 23.6%. However, the relatively low carrier mobility within the organic subcell limits the short-circuit current density and fill factor (FF), resulting in an efficiency deficit. Thermal deformation of organic molecular chains has been identified as the underlying cause of this stability gap. Nevertheless, a key comparative strength lies in their solution processability on flexible substrates, granting perovskite-organic solar cells unparalleled potential for applications in bendable electronics.

To bridge the performance gap between perovskite-organic tandems and other technologies, this article proposes several research strategies. Addressing the efficiency limitation imposed by low organic carrier mobility could involve constructing triple-junction architectures, such as perovskite/perovskite/organic stacks, to synergistically enhance infrared light absorption and carrier transport. To mitigate the thermal instability inherent to organic materials, innovations such as developing high-mobility non-fullerene acceptors (e.g., Y6 derivatives) and incorporating crosslinked polymers could enhance thermal robustness. Finally, interfacial engineering, specifically the customization and optimization of the interconnecting layer (ICL), can minimize losses arising from energy-level misalignment and reduce thermalization losses. Future research must prioritize extending the absorption edge of organic materials beyond 1000 nm and achieving operational stability exceeding 1000 hours. Through collaborative efforts spanning chemistry and device physics, perovskite-organic tandem solar cells hold significant promise as a next-generation, low-cost, flexible photovoltaic solution.

References

- [1] Shockley, W. and Queisser, H.J. (1961). Detailed balance limit of efficiency of p–n junction solar cells. *Journal of Applied Physics*, 32(3), 510–519.
- [2] Liu, J., He, Y., Ding, L. et al. (2024). Perovskite/silicon tandem solar cells with bilayer interface passivation. *Nature*, 635, 596–603.
- [3] Chen, W., Zhu, Y., Xiu, J. et al. (2022). Monolithic perovskite/organic tandem solar cells with 23.6% efficiency enabled by reduced voltage losses and optimized interconnecting layer. *Nat Energy*, 7(3), 229–237.
- [4] National Renewable Energy Laboratory. (n.d.). Best research-cell efficiency chart. U.S. Department of Energy. Retrieved October 26, 2023, from <https://www.nrel.gov/pv/cell-efficiency.html>.
- [5] Brinkmann, K.O., Wang, P., Lang, F. et al. (2024). Perovskite–organic tandem solar cells. *Nat Rev Mater*, 9, 202–217.
- [6] Eperon, G. E., Horantner, M. T. and Snaith, H. J. (2017). Metal halide perovskite tandem and multiple - junction photovoltaics. *Nature Reviews Chemistry*, 1, 95.
- [7] Zhang, M., Zhu, Z., YU, X., Yu, T., Lu, D., Li, S., Zhou, S. and Yang, H. (2023) Research progress of high-efficiency double-junction perovskite tandem solar cells. *Acta Materiae Compositae Sinica*, 40(2), 726-740.
- [8] Wang, W., Wang, J., Zheng, Z. and Hou, J. (2020). Research progress of tandem organic solar cells. *Acta Chimica Sinica*, 78(4), 382–396.
- [9] Lin, Y., Wang, J., Zhang, Z.G., Bai, H., Li, Y. and Zhu, D., et al. (2015). An electron acceptor challenging fullerenes for efficient polymer solar cells. *Advanced Materials*, 27(7), 1170-1174.
- [10] Jost, M., Al-Ashouri, A., Getautis, V., Schlattmann, R., Kasparavicius, E. and Kodalle, T., et al. (2022) Perovskite/cigs tandem solar cells: from certified 24.2% toward 30% and beyond. *ACS Energy Letters*, 7(4), 1298-1307.
- [11] Xie, Y.M., Niu, T., Yao, Q., Xue, Q., Zeng, Z. and Cheng, Y., et al. (2022). Understanding the role of interconnecting layer on determining monolithic perovskite/organic tandem device carrier recombination properties. *Journal of Energy Chemistry*, 71, 12-19.
- [12] Snaith, H. J. and Petrozza, A. (2013). Perovskite solar cells: Efficiency, stability, and scalability. *Energy and Environmental Science*, 6(8), 2393-2403.
- [13] Li, X. and Zhang, Y. (2023). Enhancement Strategies for Fill Factor and Efficiency Analysis in Tandem Solar Cells. *Journal of Solar Energy Research*, 10(2), 123 - 135.
- [14] Wu, X., LIU, Y. and QI F, et al. (2021). Improved stability and efficiency of perovskite/organic tandem solar cells with an all- inorganic perovskite layer. *Journal of Materials Chemistry A*, 9(35), 19778-19787.
- [15] Sahli, F., Jérémie, W., Kamino, B. A., Bruninger, M. and Ballif, C. (2018) Fully textured monolithic perovskite/silicon tandem solar cells with 25.2% power conversion efficiency. *Nature Materials*, 17(9).
- [16] Lin, R., Xiao, K., Qin, Z. et al. (2019) Monolithic all-perovskite tandem solar cells with 24.8% efficiency exploiting comproportionation to suppress Sn(II) oxidation in precursor ink. *Nat Energy* 4, 864–873.
- [17] Zhao, D., Chen, C., Wang, C. et al. (2018) Efficient two-terminal all-perovskite tandem solar cells enabled by high-quality low-bandgap absorber layers. *Nat Energy* 3, 1093–1100.

- [18] Todorov, T., Gershon, T., Gunawan, O., Lee, Y., Sturdevant, C. and Chang, L., et al. (2015). Monolithic perovskite-cigs tandem solar cells via in situ band gap engineering. *Advanced Energy Materials*, 5(23).
- [19] Chen, Q., Yang, N., Zheng, G. H. J., Pei, F., Zhou, W., Zhang, Y., Li, L., Huang, Z., Liu, G., Yin, R., Zhou, H., Zhu, C., Song, T. L., Hu, C., Zheng, D., Bai, Y., Duan, Y., Ye, Y., Wu, Y. and Chen, Y. (2024). Nuclei engineering for stable perovskite/silicon tandems. *Science*, 385(6708), 554-560.
- [20] Yu, Z., Yang, Z., Ni, Z. et al. (2020) Simplified interconnection structure based on C60/SnO₂-x for all-perovskite tandem solar cells. *Nat Energy* 5, 657–665.
- [21] Li, L., Wang, Y., Wang, X. et al. (2022). Flexible all-perovskite tandem solar cells approaching 25% efficiency with molecule-bridged hole-selective contact. *Nat Energy* 7, 708-717.
- [22] Tong, J., Song, Z., Kim, D. H., Chen, X., Chen, C., Palmstrom, A. F., et al. (2019). Carrier lifetimes of >1 microseconds in Sn-Pb perovskites enable efficient all-perovskite tandem solar cells. *Science*, 364(6439), 475-479.